

# Simulation Machining of Hardened Gear Shaping and Finite Element Analysis

Yan Li

University of Shanghai for Science and Technology

Zhonghou Wang (✉ [wangusst1@163.com](mailto:wangusst1@163.com))

University of Shanghai for Science and Technology

Zhongyuan He

University of Shanghai for Science and Technology

---

## Original Research

**Keywords:** cylindrical spur gear, simulation machining, gear shaping, high precision mesh

**Posted Date:** February 3rd, 2021

**DOI:** <https://doi.org/10.21203/rs.3.rs-182878/v1>

**License:** © ⓘ This work is licensed under a Creative Commons Attribution 4.0 International License.

[Read Full License](#)

---

---

## Simulation Machining of Hardened Gear Shaping and Finite Element Analysis

Yan Li, Zhonghou Wang, Zhongyuan He

Zhonghou Wang: wangusstl@163.com

School of Mechanical Engineering, University of Shanghai for Science and Technology, 516,  
Jungong Road, Shanghai, 200093, China

**Abstract:** Existing simulation processing methods are difficult to obtain the tooth surface that is close to the actual processing. This paper proposes a high-precision simulation processing method for hard tooth surface gearing. Through the establishment of a high-precision cutter and tooth blank geometric model, analysis of the kinematics principle and meshing relationship between the cutter and tooth blank, combined with the functions of rotation, translation and Boolean operation in the 3D software, the high-precision shaping simulation processing of hardened gears is realized. By measuring the normal distance between the standard involute and the gear tooth profile, the tooth surface error analysis is completed. The simulation model is reconstructed, and the models are analyzed by finite element method (FEM) respectively, and the effectiveness of the method in this paper is verified by comparing the analysis results.

**Keywords:** cylindrical spur gear; simulation machining; gear shaping; high precision mesh

### 1 Introduction

Gear shaping is a widely used gear machining method<sup>[1]</sup>. For multi-connected gears, inner gears, and other special gears, gear shaping has its unique advantages.

For double gear with compact structure, the pinion gear can't be ground after heat treatment, and due to the influence of heat-treatment deformation, the accuracy of pinion gear can't be guaranteed, and the use of hardened gear shaping should be the only feasible method<sup>[2]</sup>.

At present, the tooth surface hardness that can be machined by the hardened gear shaping process is HRC45-64, the precision is 6-7, and the roughness  $R_a$  is 0.4-0.8 $\mu$ m.

However, for gears with hardened gear shaping, the surface will inevitably leave a machined texture, that is, tooth surface tool marks. During the meshing process, the protrusions formed by the tooth surface tool marks will exceed the thickness of the lubricating film and cause direct contact. Eventually, local contact stress is too large, and micropitting corrosion is formed<sup>[3]</sup>. Micropitting will gradually evolve into destructive pitting and even lead to tooth surface failure. If we need to analyze this kind of tooth surface contact conditions, we need to establish a gear model that matches the actual tooth surface.

Researchers have established simulation

machining models of gear shaping and predicted the cutting force through computer-aided design. Tsay et al.<sup>[4]</sup> proposed a complete geometric mathematical model of involute gears based on gear shaping according to the tool tooth profile theory and gear shaping motion model, and the effects of the cutter parameters on the generated tooth profile are investigated and illustrated with computer simulation. Fetvaci<sup>[5]</sup> obtained the mathematical model of asymmetric involute gears processed by gear shaping according to gear theory and geometric principles. In addition, the motion path in gear shaping is simulated, and the geometry of undeformed chips is obtained for further cutting force analysis. Erkorkmaz et al.<sup>[6]</sup> proposed a prediction model for the shaping cutting force of spur gears, the discretization method is used to calculate the stress value of a single node in the gear shaping process, and then the node stress value is correlated with the chip geometry, and the overall cutting force prediction is finally realized. Katz et al.<sup>[7]</sup> proposed a comprehensive model of gear shaping, including spur gear, internal gear, helical gear shaping kinematics model, and cutting force prediction model. Nan<sup>[8]</sup> established the gear blank and tool model in NX and completed the simulation machining of spur gears according to the principle of gear shaping. By extracting the tooth surface

from the simulation model, the accurate modeling of the gear was completed, but the accuracy of the model was not discussed. Pu et al.<sup>[9]</sup> simulated gear hobbing based on the CATIAV5, but the purpose of the simulation was only to establish a three-dimensional accurate model of the gear tooth profile, without considering the actual machining tooth surface condition. Kawalec et al.<sup>[10]</sup> used the finite element method to study the tooth root strength of gears processed by gear shaping. This paper proposes a high-precision gear shaping simulation method. First, an accurate model of the shaper cutter and the tooth blank is established. Then analyzed the spatial movement relationship between the gear shaper cutter and the gear blank, combined with the commands of translation, rotation, Boolean operation in the 3D software and secondary development functions, completed the high-precision shaping simulation processing of cylindrical spur gears. A high-precision gear shaping simulation model is obtained. This paper only completed the simulation processing of spur cylindrical external gears, but many of the methods are also applicable to internal gears and helical gears.

The rest of this paper is as follows: Section 2 introduces the gear shaping processing method and vector modeling of gear shaping movement; Section 3 introduces the concrete realization of gear shaping simulation processing; Section 4 is the verification and analysis of simulation tooth surface accuracy; Finally, Section 5 is the conclusion.

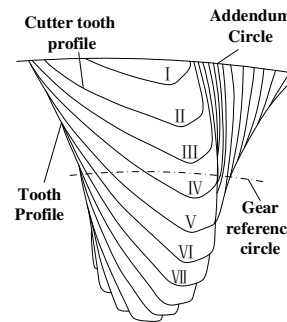
## 2 Gear shaping and machining motion model

Gear shaping is the use of generative principles to machine gears. The process of machining a spur gear can be regarded as a discontinuous meshing process of a pair of spur gears. The teeth in one of the gears are given the same rake angle  $\alpha$  and back angle  $\beta$  to form a cutting edge, and the gear can be regarded as a gear shaper cutter and another gear can be regarded as a tooth blank to be machined. As shown in Fig.1a, the

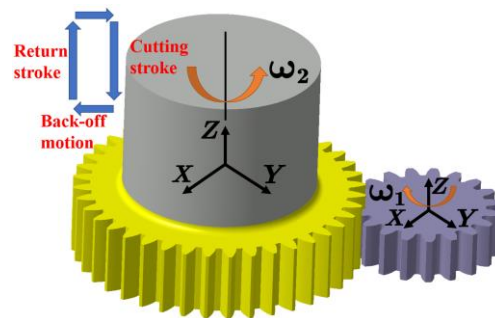
teeth in the gear shaper cutter successively occupy positions I, II, III, and IV in the tooth blank, so that a complete involute tooth shape can be enveloped on the tooth blank by reciprocating.

### 2.1 Gear shaping motion model

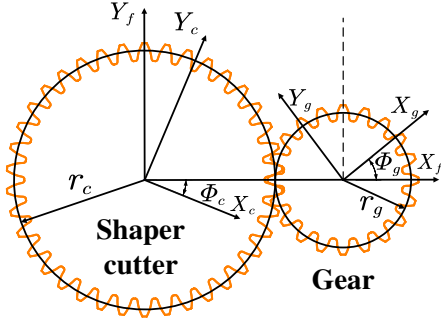
The gear shaping movement process of the spur gear is shown in Fig.1b. In gear shaping, the main movement is the high-speed reciprocating linear movement of the gear shaper cutter in the axial direction. At present, the linear speed of ordinary high-speed steel tools is usually 30-50m/min. Generating motion is pure rolling between gear shaper cutter and gear blank. The gear shaper cutter rotates around its axis at an angular velocity  $\omega_2$ , and the gear blank also rotates opposite to the gear shaper cutter around its axis at an angular velocity  $\omega_1$ . The retraction movement is the moving away of the cutter along with the radial direction of the tooth blank; the feed movement is the radial feeding movement of the gear shaper cutter along with the tooth blank, In the finishing machining of hard tooth surface gear shaping, the radial feed is generally not more than 0.12mm/str, and the rotary feed is not more than 0.1mm/str.



(a) Tooth envelope



(b) Basic kinematics of gear shaping



(c) Kinematic relationship between the shaper cutter and the machined gear

Fig. 1. Principle movements and geometries in gear shaping

Figure.1c shows the coordinate relationship between the gear shaper cutter and the gear blank, the right-handed coordinate systems are considered. The coordinate system  $S_f(X_f, Y_f)$  is the reference coordinate system, the coordinate system  $S_c(Y_c, X_c)$  denotes the gear blank coordinate system, and the coordinate system  $S_g(Y_g, X_g)$  represents the shaper cutter coordinate system. In the generation process, the cutter rotates through an angle  $\theta_c$ , while the gear blank rotates through an angle  $\theta_g$ . The relationship between the angles  $\theta_c$  and  $\theta_g$  is  $\theta_g = (Z_c/Z_g)\theta_c$ , where  $Z_c$  is the number of teeth of the cutter and  $Z_g$  denotes the number of teeth of the generated gear.  $r_c$  and  $r_g$  donate the index circle radius of the gear shaper cutter and the machined gear respectively. The method of homogeneous coordinate transformation is a powerful tool for studying the motion of a rigid body among the different coordinate systems. The coordinate transformation matrix from coordinate system  $S_c$  to  $S_g$  is shown as follows:

$$M_{gc} = \begin{bmatrix} \cos(\Phi_c + \Phi_g) & \sin(\Phi_c + \Phi_g) & -(r_c + r_g)\cos\Phi_g \\ -\sin(\Phi_c + \Phi_g) & \cos(\Phi_c + \Phi_g) & (r_c + r_g)\sin\Phi_g \\ 0 & 0 & 1 \end{bmatrix} \quad (2-1)$$

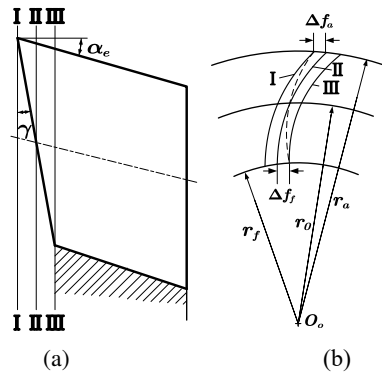
According to the theory of gearing<sup>[11]</sup>, the mathematical model of the generated gear tooth surface is a combination of the meshing equation

and the locus of the rack cutter surfaces. The locus of the shaper cutter surface, expressed in coordinate system  $S_g$ , can be determined as follows:

$$\mathbf{R}_g^i = [M_{gc}] \mathbf{R}_c^i, (i = 1, \dots, 6) \quad (2-2)$$

## 2.2 Establishment of gear shaper cutter and gear blank model

When the gear shaper cutter cuts the gear, the track surface of the cutting edge's up and down movement should mesh with the gear to be machined, the projection of the cutting edge on the end surface should be an involute curve so that there is no error on the tooth surface. As shown in Fig.2a and 2b, when the rake angle  $\gamma = 0^\circ$  of the gear shaper cutter, the tooth profile of the rake face of the gear shaper cutter is involute, and there is no error. When the rake angle  $\gamma > 0^\circ$  of the gear shaper cutter, the rake surface is a conical surface, and the projection of the cutter on the end surface is no longer an involute. Taking the involute tooth profile in the section II-II as the reference, the thickness of the tooth tip will increase in section I-I. Similarly, the thickness of the tooth will decrease in section III-III, which is equivalent to the pressure angle of the reference circle will be reduced, resulting in a larger tooth profile error. In Fig. 2,  $r_a$  is the addendum circle radius,  $r_f$  is the root circle radius,  $r_0$  is the reference circle radius, and  $\alpha_e$  is the top edge relief angle.



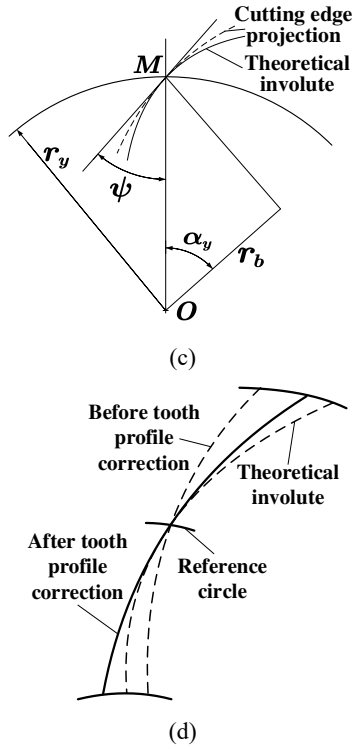


Fig. 2. Gear shaper cutter tooth profile: (a)(b) Tooth profile error, (c) Tooth Angle correction, (d) Tooth projection.

To reduce the tooth profile error, the profile angle of the gear shaper cutter is usually corrected in such a way that the reference circle pressure angle of the tool blade projection is equal to the gear reference circle pressure angle. That is, the tooth profile angle of the gear shaper cutter is corrected so that the tooth profile angle  $\alpha_0$  of the gear shaper cutter and the gear reference circle pressure angle  $\alpha$  are not equal, but the tangent of the tool blade projection on the reference circle coincides with the theoretical involute tangent, so we can get the original tooth profile angle of the shaper cutter. As shown in Fig. 2c, point M is any point on the blade curve,  $r_y$  is the radius at point M,  $r_b$  is the radius of the shaper cutter base circle, and  $\psi$  is the angle between the tangent and the radial passing through the M point. According to the gear cutter principle:

$$\tan \psi = \tan \alpha_y - \frac{r_y}{r_0} \tan \gamma \tan \alpha_0 \tan \epsilon \quad (2-3)$$

Let the angle  $\psi$  of the projection curve of the

tool edge at the reference circle be equal to the pressure angle  $\alpha$  of the theoretical involute:

$$\psi = \alpha, r_y = r_0, \alpha_y = \alpha_0 \quad (2-4)$$

$\alpha_0$  can be obtained as follows:

$$\tan \alpha_0 = \frac{\tan \alpha}{1 - \tan \gamma \tan \alpha_e} \quad (2-5)$$

$\alpha_0$  is the original tooth profile angle of the cutter. The tooth profile projection before and after the correction is shown in Fig. 2d.

After obtaining the original tooth profile angle of the cutter, according to the parameters shown in Tab. 1, we established an accurate model of the shaper cutter, as shown in Fig. 4a.

Tab. 1. Cutter and workpiece geometry.

Module [mm]	No. of teeth	Modification coefficient	Rake angle [deg]	Relief angle [deg]	Tip Radius [mm]
Cutter geometry					
2	38	-0.5	0.2	5	6
Module [mm]	No. of teeth	Pressure angle [deg]	Width [mm]	Modification coefficient	
2	20	20	10	-0.2	
Workpiece geometry					

Measure the normal distance between the projection of the end face of the cutting edge of the gear shaper cutter and the standard involute, the resulting shape error data of the shaper cutter is shown in Fig. 3. Among them, the left side is the tip part of the cutter.

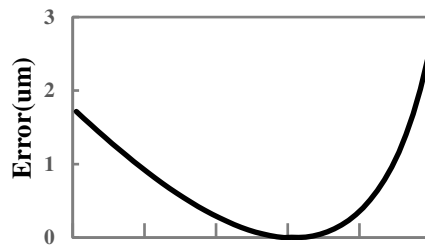


Fig. 3. Cutter tooth profile error

Corresponding to Fig. 2d, the shape projection of the shaper cutter protrudes slightly at the top and root of the tooth.

According to the gear tool design manual<sup>[12]</sup>, the error between the projection of the cutting edge and the theoretical involute as follows:

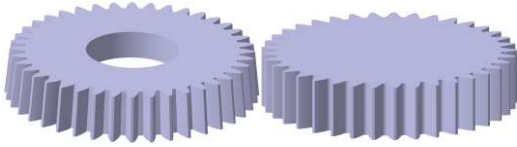
$$\begin{aligned} \Delta\theta_y &= (\text{inv}\alpha_{y0} - \text{inv}\alpha_y) \\ &- (\text{inv}\alpha_0 - \text{inv}\alpha) - (r_y - r_0)K \quad (2-6) \\ \Delta f_y &= r_y * \Delta\theta_y \end{aligned}$$

Where:

$$K = \frac{\tan\gamma \tan\alpha_0 \tan\alpha_e}{r_0} \quad (2-7)$$

It is obtained that the tooth profile error at the tooth tip is 1.8019um and the tooth root is 2.6214um, which is basically consistent with the data of our model, thus verifying the correctness of the gear shaper cutter model.

To reduce the amount of calculation while ensuring the accuracy of the simulation, in the gear shaping simulation, we simplified the gear shaper cutter model with rake and back angles. We projected the high-precision gear shaper cutter model on the end surface and stretched the curve obtained by the projection axially to obtain a simplified gear shaper cutter model that meets the simulation requirements, as shown in Fig.4b.



(a) The accurate model (b) The simplified model

Fig.4 The model of Gear shaper cutter

### 3 Simulation process of gear shaping

The simulation processing flow chart of gear shaping is shown in Fig.5. Firstly, a simplified model of gear shaper cutter and a model of gear blank were established in 3D modeling software. Then the simplified model of the cutter and the model of the gear blank were assembled in the assembly design environment. Finally, the position adjustment and Boolean operation between the cutter and the gear blank were driven in the part design environment.

In the simulation processing, we simplified the gear shaping movement, only retain the rotary movement of the cutter and the gear blank. Each time the above-mentioned spatial position transformation and Boolean operation are performed, it can be regarded as that the tooth

blank model is cut by the cutter model once.

In the simulation process, we repeated the above steps until the entire gear was cut out, thus completing the entire modeling process.

In the entire cutting process, due to the need for a large number of position adjustments and Boolean operations, the use of the macro-function in the CATIA software can realize the automation of the entire simulation processing.

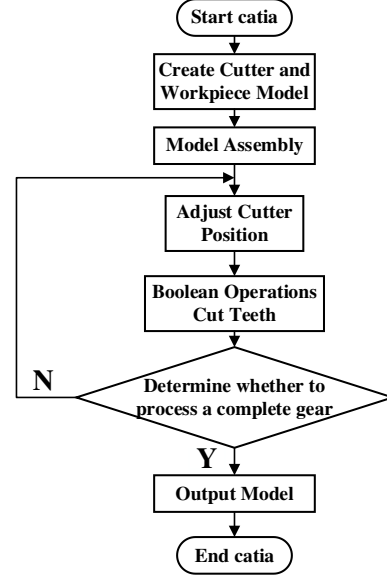


Fig. 5.The flow chart of gear shaping simulation.

The main control factors in simulation processing are the number of cycle feeds  $n$  and the circumferential feed  $\Delta\theta$ . The relationship between them as follows:

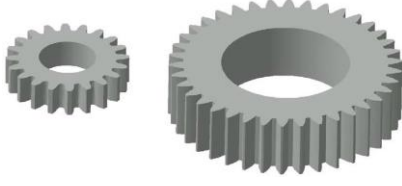
$$n = \pi * m * z / \Delta\theta \quad (3-1)$$

The number of cycles  $n$  depends on the circumferential feed  $\Delta\theta$ . The smaller the circumferential feed, the higher the machining accuracy. In the simulation process, we chose to use three different circumferential feeds, which are 0.1mm/str, 0.2mm/str, and 0.3mm/str, which are consistent with the actual parameters in the precision gear machining process<sup>[2]</sup>.

The simulation process is shown in Fig.6.



(a) Before processing (b) During processing



(c) After processing

Fig. 6. Gear shaping process

#### 4 Verification of tooth surface accuracy

##### 4.1 Tooth surface error

To study the accuracy of the tooth surface of the simulation model, it is necessary to compare the model tooth surface with the standard involute. The involute equation can be written as

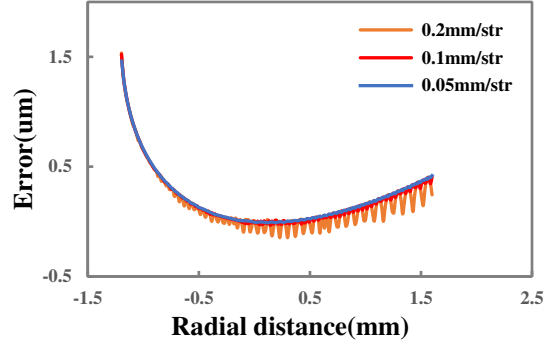
$$\begin{aligned} x &= r_b \cdot \sin u - r_b \cdot u \cdot \cos u \\ y &= r_b \cdot \cos u + r_b \cdot u \cdot \sin u \end{aligned} \quad (4-1)$$

We have obtained the theoretical involute shape and imported it into CATIA. To facilitate the comparison of the tooth surface error under different circumferential feeds, the midpoint of the tool mark closest to the reference circle was selected to intersect the involute.

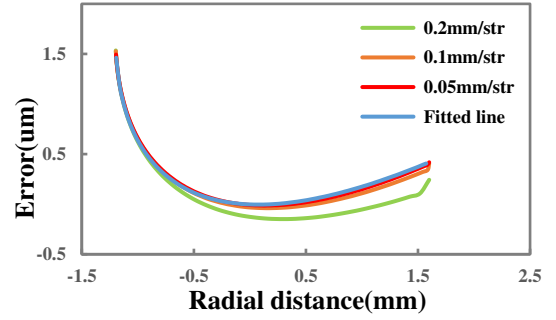
During the comparison, we performed two measurements:

1. Measure the normal distance between the tooth surface of the simulation model and the theoretical involute, and show the true error of the tooth surface of the simulation model;
2. Measure the normal distance between the tool mark line of the simulation model and the theoretical involute, and visually display the maximum error of the simulated machining tooth surface;

After sorting the above data, the error curve between the simulation model tooth surface and the theoretical involute tooth surface can be obtained as shown in Fig.7a. Among them, the left side is the part close to the tooth root. The abscissa is the radial distance between the tool mark line and the reference circle, and the ordinate is the normal distance between the gear tooth surface and the standard involute.



(a) Tooth surface error of simulation model



(b) Tooth surface error of tool mark line

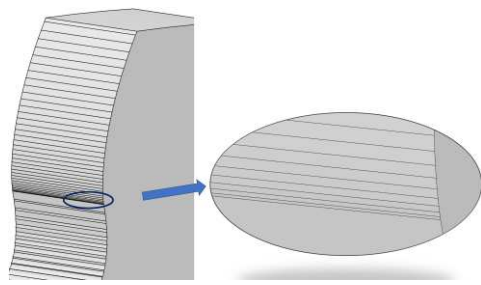
Fig. 7. Error curve

We took the midpoint of each tool mark and then reconstructed the tooth surface using B-spline interpolation. The standard involute and the reconstructed spline curve intersected at the reference circle. The normal distance between the spline curve and the involute was measured, and the error curve between the reconstructed tooth surface and the standard involute as shown in Fig. 7b was obtained.

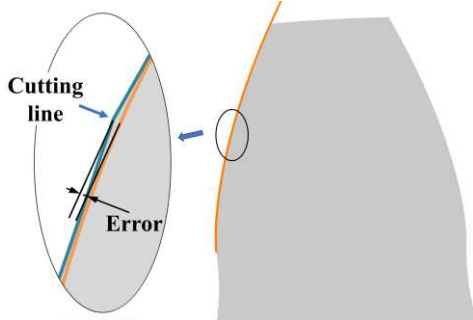
##### 4.2 Error analysis

Fig.7b intuitively shows the distribution of the error value on the tooth surface. The error value gradually increases in the direction of the tooth tip and the tooth root based on the reference circle. This also coincides with the slightly convex projection of the cutting edge of the gear shaper.

Comparing the error curves under different circumferential feeds, it can be found that the errors of the gear models processed at different feeds are basically the same in the part near the tooth root. The reason analysis is that the tool marks near the tooth root of the gear are dense so that the point error on the tool mark line is small under different feed rates. As shown in Fig.8a.



(a) 0.3mm/str working conditions of the cutter mark line



(b) Tool mark line error measurement

Fig. 8. Tool marks

In the area of the reference circle and the tooth tip, when the circumferential feed is 0.1mm/str, it can be found that compared with the fitted model, the error basically tends to zero. However, as the circumferential feed increases, the error tends to be negative, which is reflected in the model as the tool mark line is protruding from the involute line. The reason is that the point on the tool mark line is the point with the largest error on the tooth surface, which leads to a large error in the measured tooth surface, as shown in Fig.8b.

As shown in Fig.7b, there is a small jump in the error curve of the tooth tip, and the error after the jump is close to the error of the fitting curve at this point. This is because the last measurement is not a point on the normal tool mark line, but a point on the addendum circle, which leads to a reduction in the measurement error. As the circumferential feed increases, the jump amplitude may also increase.

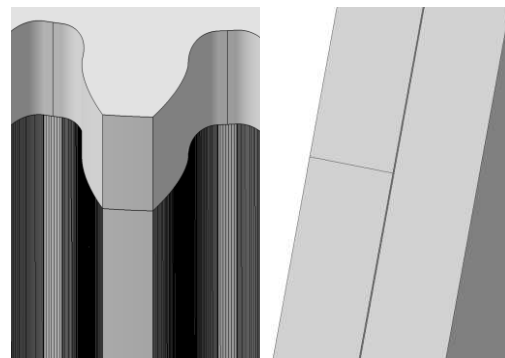
In summary, as the circumferential feed step increases, the error between the simulation model tooth surface and the theoretical involute also increases.

In actual processing, the gear shaper cutter and

the gear blank carry out relatively discontinuous meshing movement. As the circumferential feed of the gear shaper cutter decreases, the more times the tooth groove is enveloped, the smoother the tooth surface and the higher the accuracy.

#### 4.3 FEM of the simulation model

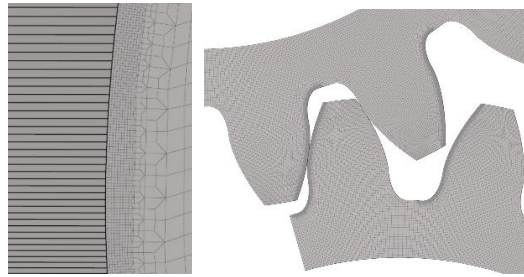
We reconstructed the simulation model with a typical circumferential feed of 0.1mm/str into a model without tool marks using B-spline interpolation. There are slight fluctuations between the reconstructed model tooth surface and the simulation model, as shown in Fig.9.



(a) Comparative model (b) Enlarged model

Fig.9. Simulation model and reconstruction model

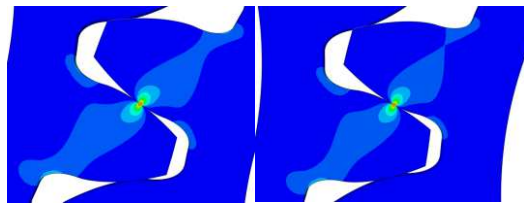
The simulation model and the reconstructed model were imported into software respectively, and high-precision meshing was performed on them. The accuracy of finite element method depends on the mesh size of the model, but overly precise meshes will lead to excessive consumption of computer computing power and prolong calculation time while obtaining accurate results<sup>[13]</sup>. Therefore, we chose to refine the mesh of the gear meshing area, while the remaining areas are represented by larger units. To reflect the influence of the tool mark line in the finite element solution, nodes need to be arranged at the tool mark line, and the mesh at the tool mark line is shown in Fig.10a. The meshed model was installed as standard, as shown in Fig.10b.



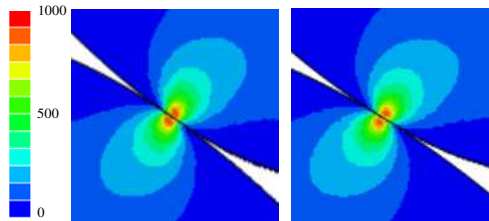
(a) Meshes on milling (b) Meshes of the simulation model

Fig.10 Mesh model of the gear

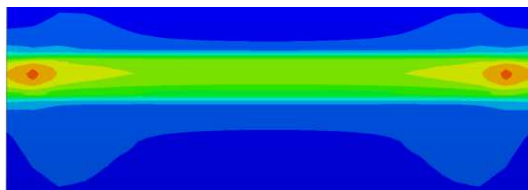
The above models were analyzed by finite element method. The material is 40Cr. When the resistance torque given to the simulation model and the reconstruction model is  $25 \text{ N} \cdot \text{m}$ , the simulation result is shown in Fig.11.



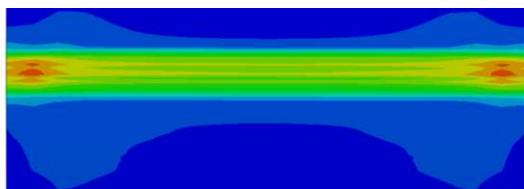
(a) (b)



(c) (d)



(e)



(f)

Fig.11 Contact stress comparison

Extract the maximum contact stress during gear meshing, as shown in Fig.12. According to the results of the finite solution, the maximum contact stress on the tooth surface is near the node.

The maximum contact stress of the simulation model is  $1021 \text{ MPa}$ , while the reconstruction model is only  $905 \text{ MPa}$ . The maximum contact stress of the simulation model and the reconstruction model both change periodically. Compared with the reconstruction model, the maximum stress of the simulation model has increased by 20% on average, and the stress changes more frequently.

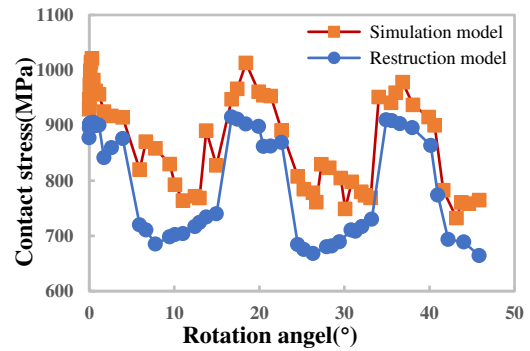


Fig.12 Curve of maximum contact stress

In practical applications, pitting corrosion first appears near the node near the tooth root, This is because the contact stress between tooth surfaces changes cyclically, and the contact stress changes most frequently near the pitch line near the tooth root. However, due to the existence of knife marks, the contact stress on the tooth surface changes frequently and the amplitude is larger than that of a smooth plane, so pitting corrosion is more likely to occur.

The existence of tool marks in actual gear shaping and gear meshing is inevitable. If only the reconstruction model of the simulation model is used in the finite element analysis, the result cannot accurately reflect the stress distribution of the gear in actual meshing. To obtain an accurate stress distribution, a gear simulation model close to the actual tooth surface is required. The simulation model obtained by the method can be as close to the actual tooth surface as much as possible. Therefore, through the finite element analysis of the simulation model obtained by this method, the contact stress distribution closest to the actual meshing can be obtained.

## 5 Conclusion

Based on the conjugate tooth surface generation processing principle and the gear shaping movement principle, this paper presents a simulation model of hard tooth surface gear shaping. By changing the circumferential feed, the simulation processing under different actual processing parameters is realized. The simulation results are compared with the theoretical involutes under the corresponding parameters, the error analysis is realized. The simulation model is reconstructed, and the simulation model and the reconstructed model are respectively solved by the finite element method. By comparing the analysis results, the validity of the simulation model obtained by this method is verified. The method in this paper is also applicable to helical gear and internal gear shaping and can provide a high-precision simulation solution for hard tooth surface gear shaping.

## References

- [1] BOUZAKIS K D, LILI E, MICHAELIDIS N, et al. Manufacturing of cylindrical gears by generating cutting processes: A critical synthesis of analysis methods [J]. *CIRP Ann-Manuf Technol*, 2008, 57(2): 676-96.
- [2] H.X. Zhao, S.Y. Bi, et al. Research on Shaper Processing of Hardened Gear Tooth [J]. *New Technology & New Process*, 2010, (03): 90-2.
- [3] BERGSTEDT E, LIN J C, OLOFSSON U. Influence of gear surface roughness on the pitting and micropitting life [J]. *Proc Inst Mech Eng Part C-J Eng Mech Eng Sci*, 2020, 234(24): 4953-61.
- [4] TSAY C-B, LIU W-Y, CHEN Y-C. Spur gear generation by shaper cutters [J]. *Journal of Materials Processing Technology*, 2000, 104(3): 271-9.
- [5] FETVACI C. Generation Simulation of Involute Spur Gears Machined by Pinion-Type Shaper Cutters [J]. *Strojnicki Vestn-J Mech Eng*, 2010, 56(10): 644-52.
- [6] ERKORKMAZ K, KATZ A, HOSSEINKHANI Y, et al. Chip geometry and cutting forces in gear shaping [J]. *CIRP Annals*, 2016, 65(1): 133-6.
- [7] KATZ A, ERKORKMAZ K, ISMAIL F. Virtual Model of Gear Shaping-Part I: Kinematics, Cutter-Workpiece Engagement, and Cutting Forces [J]. *J Manuf Sci Eng-Trans ASME*, 2018, 140(7): 15.
- [8] Y.S. Nan. UG-based simulation machining and error analysis of orthogonal spur gear shaping [D]; Taiyuan University of Technology, 2018.
- [9] T.P. Pu, J.Y. Tang. Journal of System Simulation [J]. *Journal of System Simulation*, 2008, (16): 4339-43.
- [10] KAWALEC A, WIKTOR J. Tooth root strength of spur and helical gears manufactured with gear-shaper cutters [J]. *J Mech Des*, 2008, 130(3): 5.
- [11] LITVIN F, FUENTES AZNAR A. Gear geometry and applied theory [M]. 2004.
- [12] J.Z. Yuan. Gear Tool Design [M]. National Defense Industry Press, 2014.
- [13] Y.D. Zhang, X.P. Xie, et al. Gear Contact Simulation Based on Finite Element Method [J]. *Lubrication Engineering*, 2009, 34(01): 49-51.

## Declarations

### Funding:

Supported by the National Natural Science Foundation of China (Grant No. 51875360) the Shanghai Science and Technology Commission (Grant No.: 19060502300)

### Conflicts of interest/Competing interests:

Not applicable

**Availability of data and material:** Data are available on request to the authors.

**Code availability:** Code are available on request to the authors.

### Authors' contributions:

sThis paper presents a simulation model of hard tooth surface gear shaping.

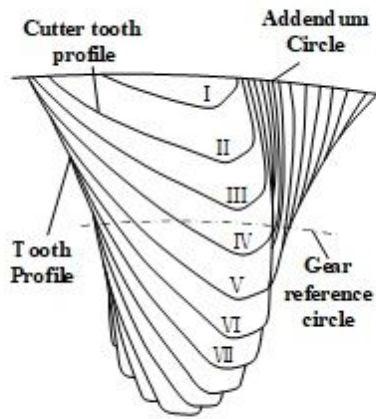
### Ethics approval.

---

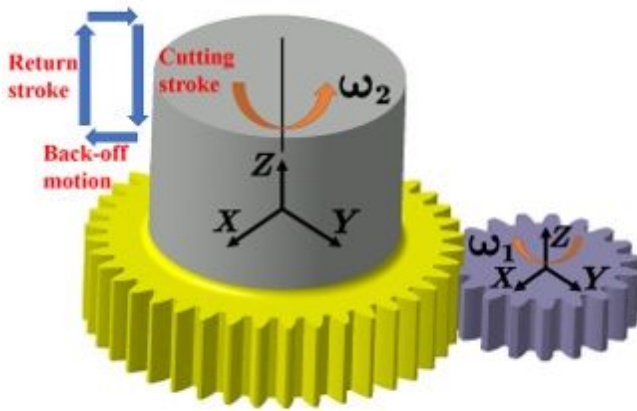
**Consent to participate.**

**Consent for publication.**

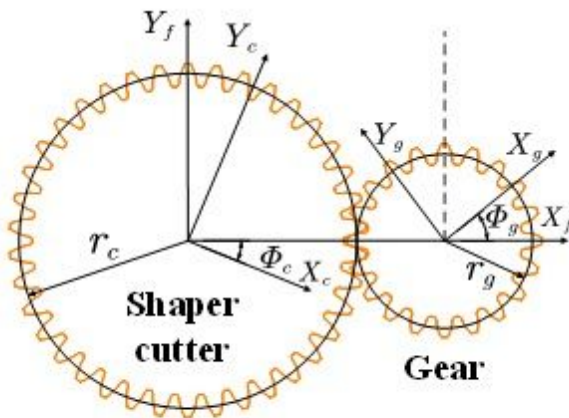
# Figures



(a) Tooth envelope



(b) Basic kinematics of gear shaping



(c) Kinematic relationship between the shaper cutter and the machined gear

Figure 1

Principle movements and geometries in gear shaping

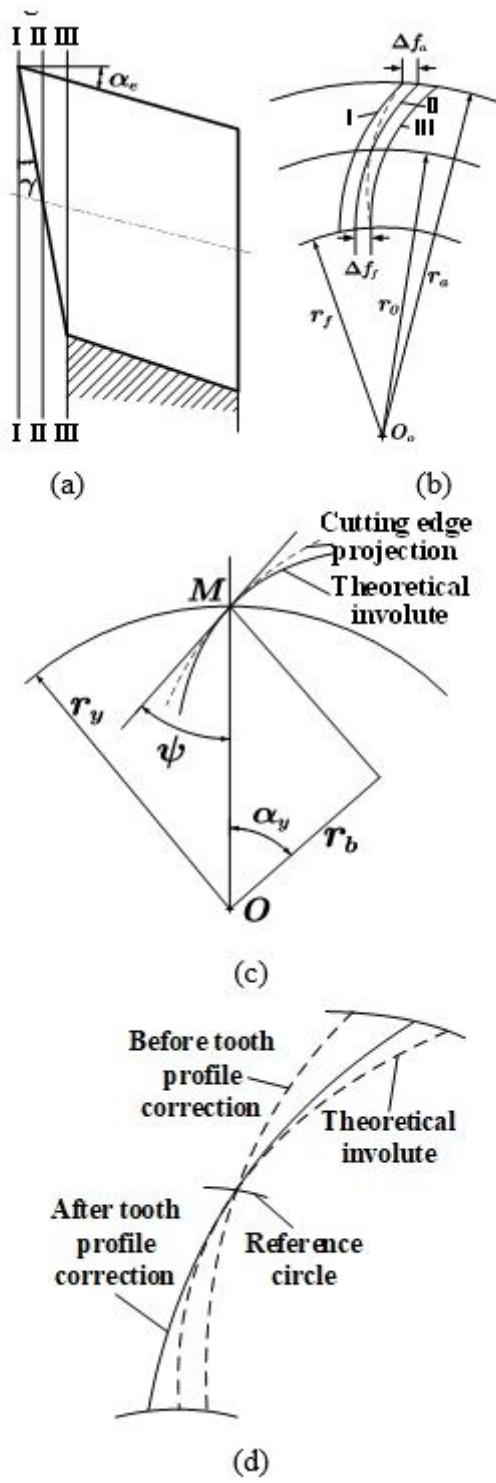


Figure 2

Gear shaper cutter tooth profile: (a)(b)Tooth profile error, (c)Tooth Angle correction, (d)Tooth projection.

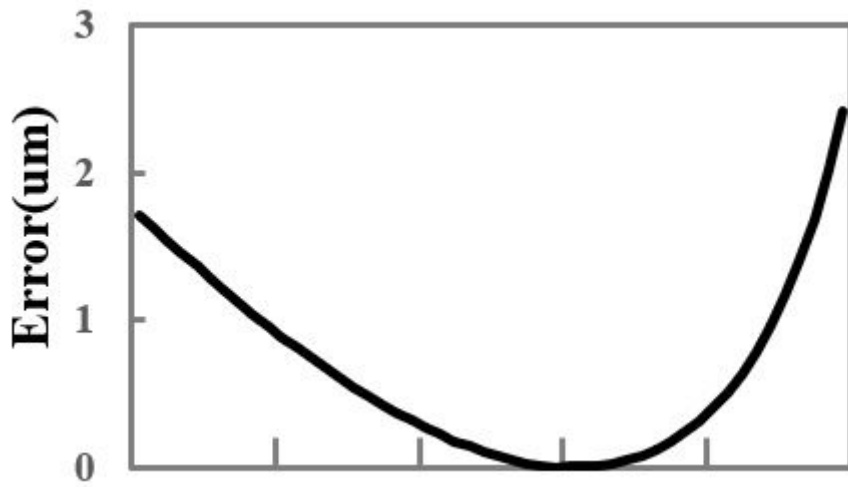
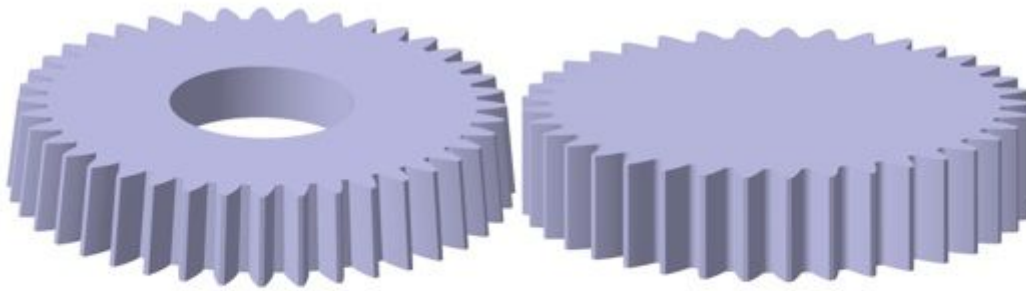


Figure 3

Cutter tooth profile error



(a) The accurate model (b) The simplified model

Figure 4

The model of Gear shaper cutter

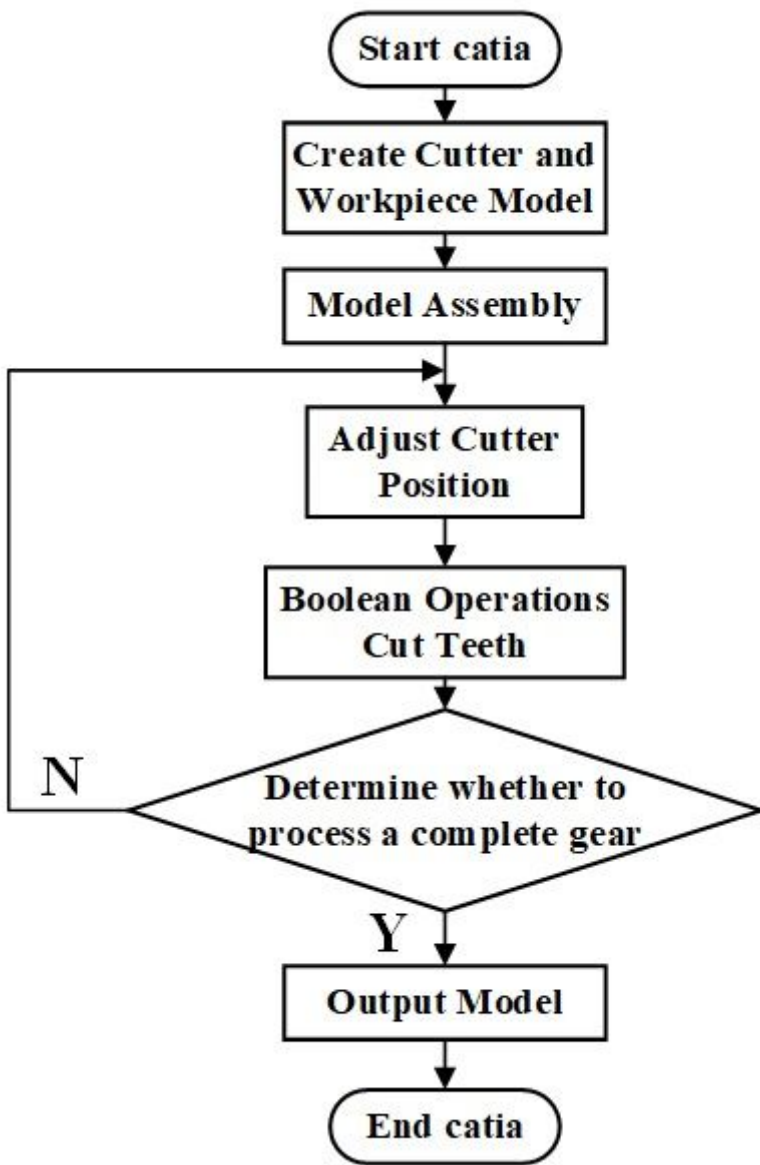
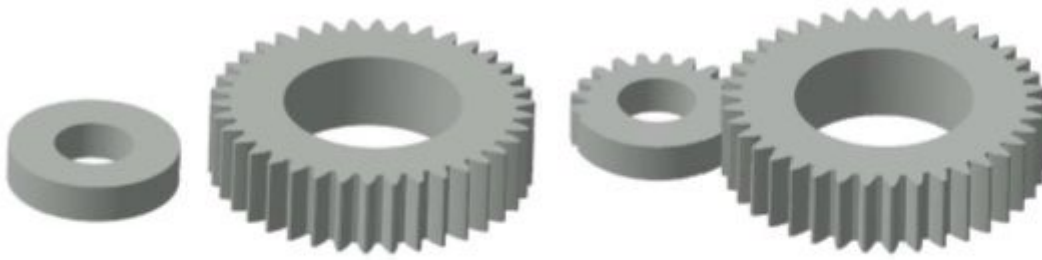
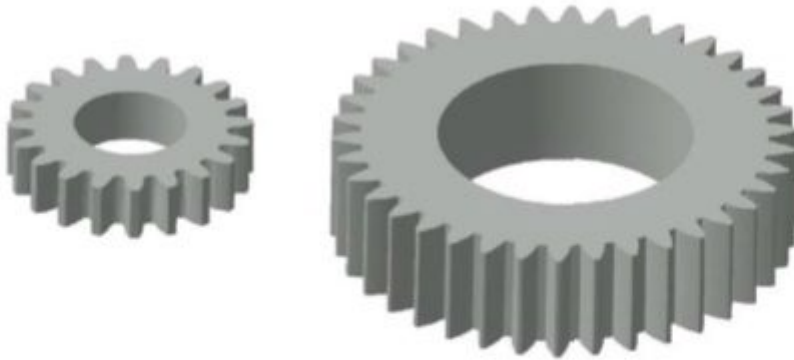


Figure 5

The flow chart of gear shaping simulation.



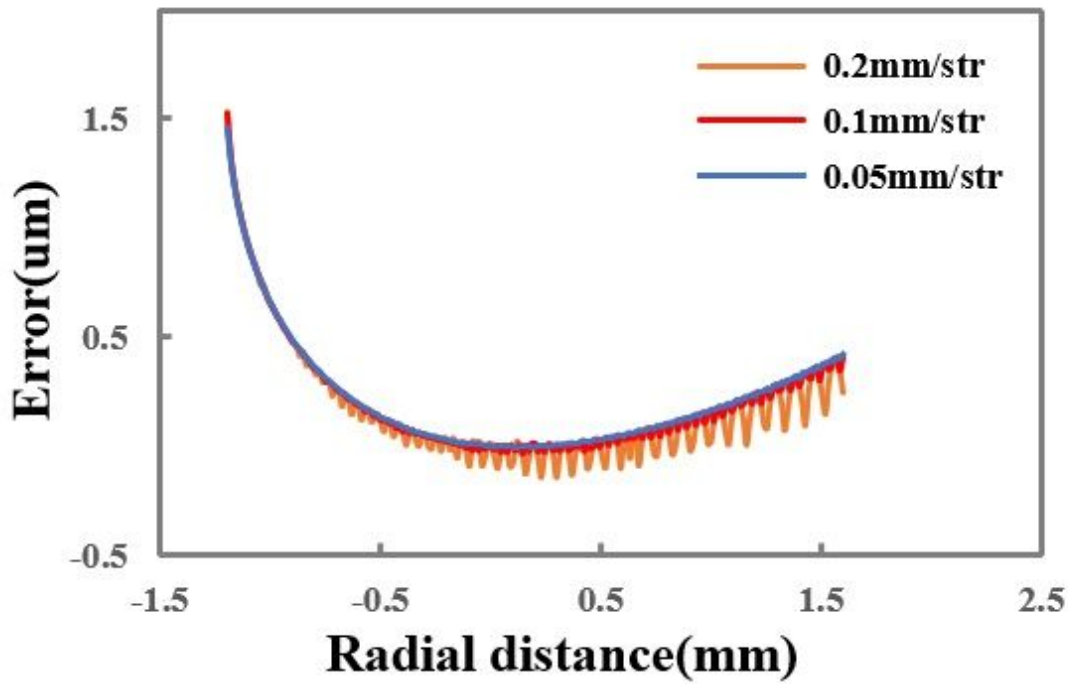
(a) Before processing (b) During processing



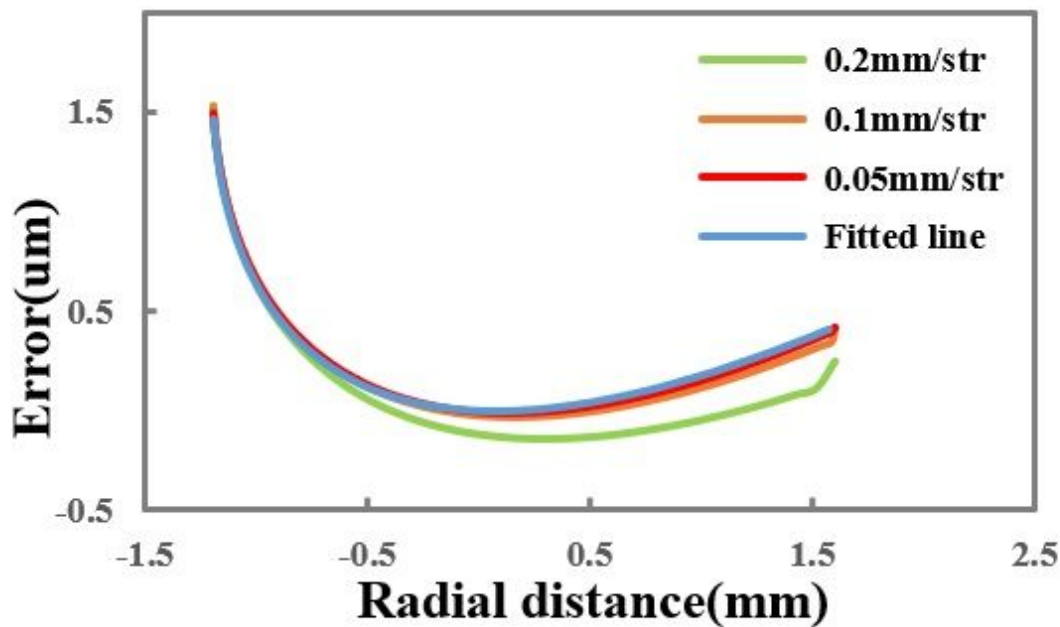
(c) After processing

**Figure 6**

Gear shaping process



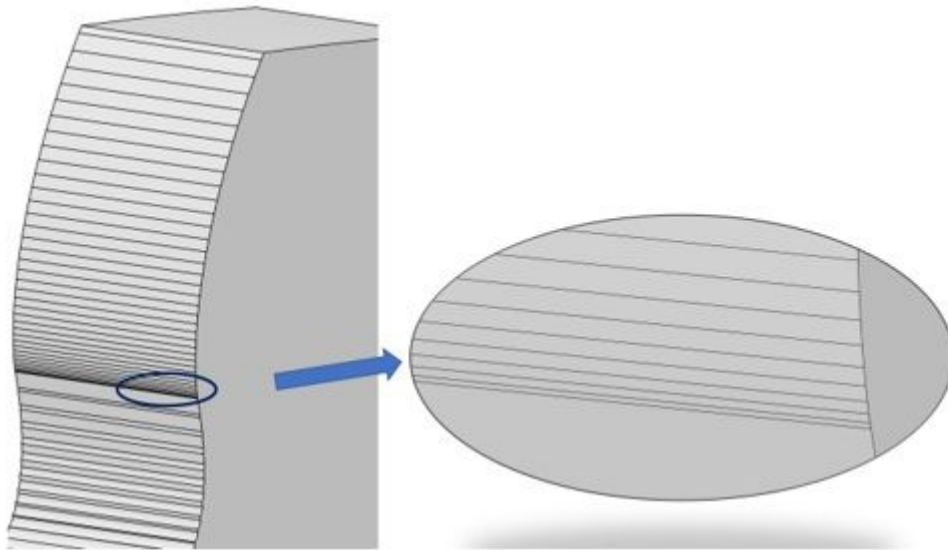
(a) Tooth surface error of simulation model



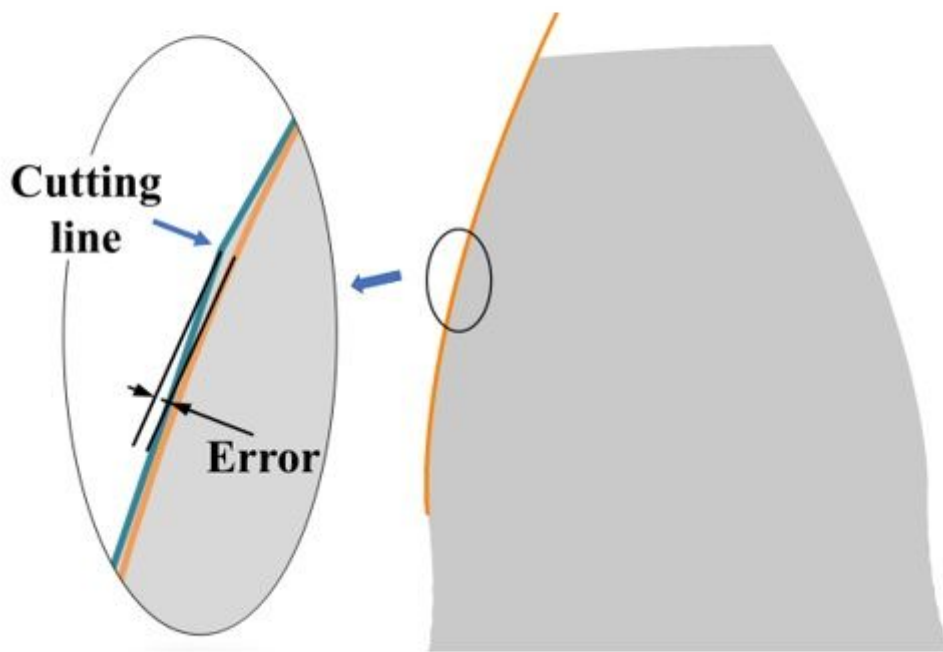
(b) Tooth surface error of tool mark line

Figure 7

Error curve



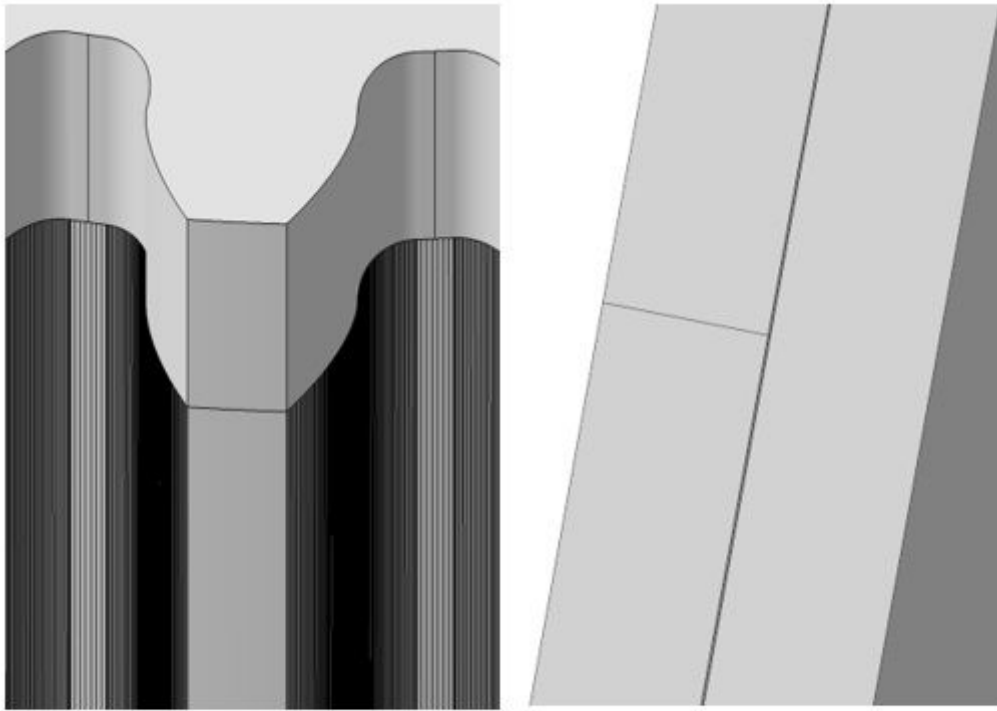
(a) 0.3mm/str working conditions  
of the cutter mark line



(b) Tool mark line error measurement

Figure 8

Tool marks

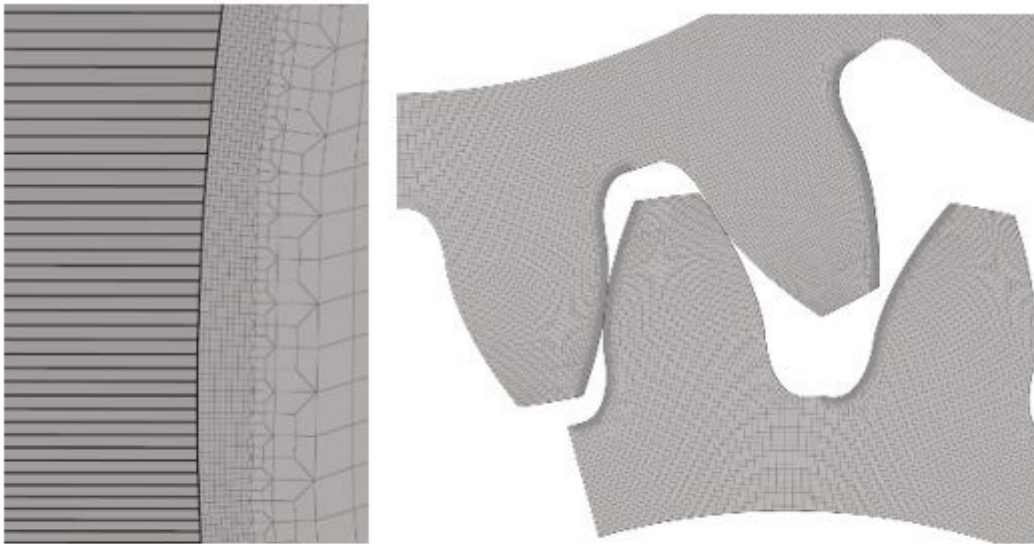


(a) Comparative model

(b) Enlarged model

**Figure 9**

Simulation model and reconstruction model

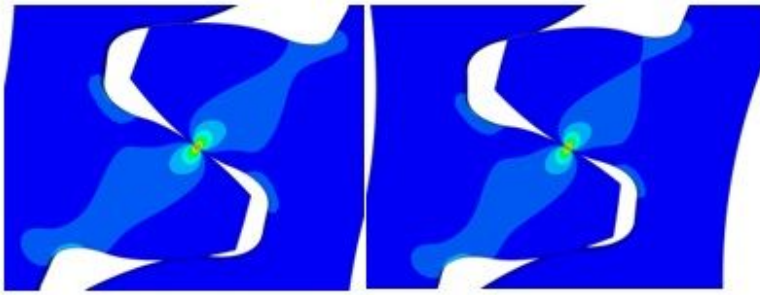


(a) Meshes on milling

(b) Meshes of the simulation model

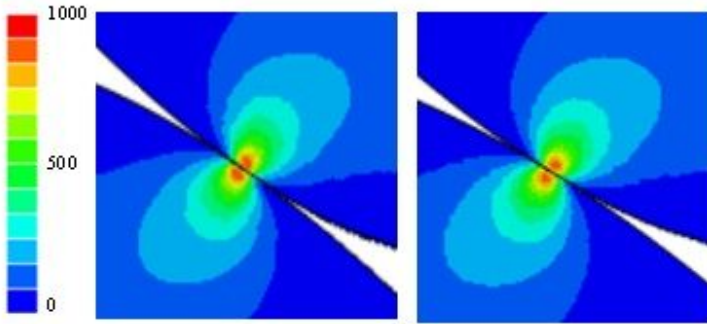
**Figure 10**

Mesh model of the gear



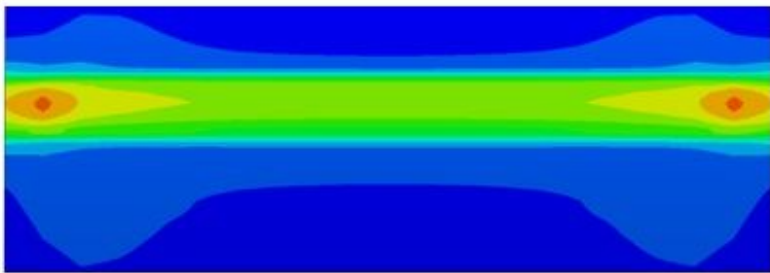
(a)

(b)

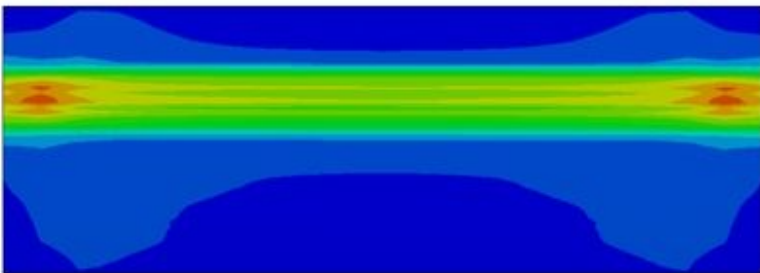


(c)

(d)



(e)



(f)

Figure 11

Contact stress comparison

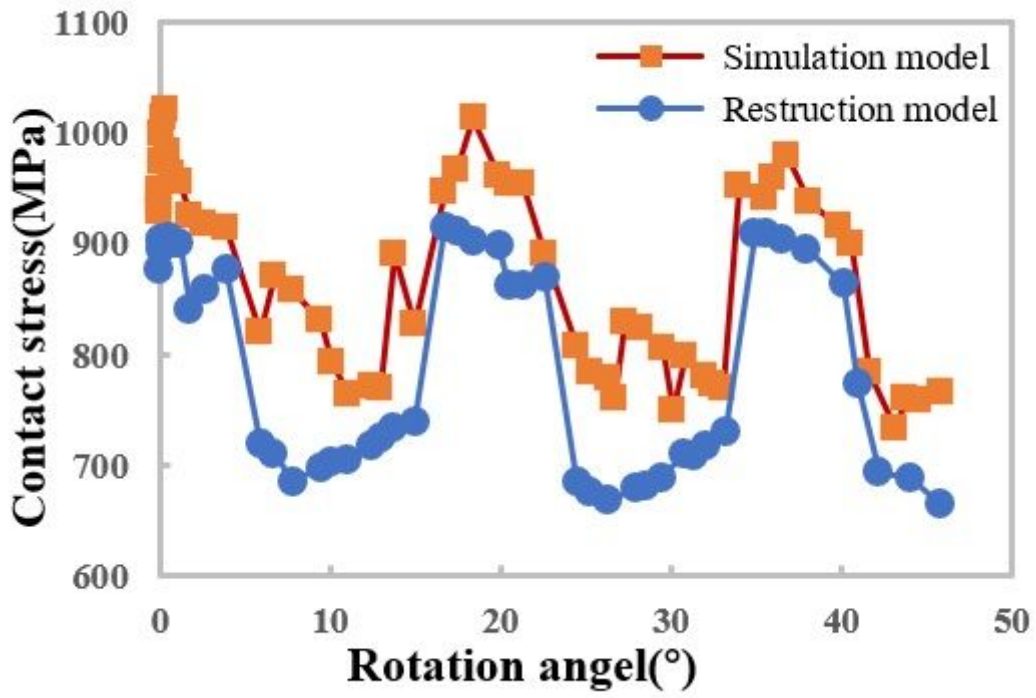


Figure 12

Curve of maximum contact stress